

# Synthesis, structure and magnetic properties of two end-on double azido bridged nickel(II) dinuclear entities incorporating *N,N,N*-coordinating tridentate reduced Schiff base ligands

Sumana Sarkar <sup>a</sup>, Amrita Mondal <sup>a</sup>, Mohamed Salah El Fallah <sup>b</sup>, Joan Ribas <sup>b</sup>,  
Deepak Chopra <sup>c</sup>, Helen Stoeckli-Evans <sup>d</sup>, Kajal Krishna Rajak <sup>a,\*</sup>

<sup>a</sup> *Inorganic Chemistry Section, Department of Chemistry, Jadavpur University, Kolkata 700 032, India*

<sup>b</sup> *Department de Química Inorgànica, Universitat de Barcelona, Diagonal 6487, 08028 Barcelona, Spain*

<sup>c</sup> *Solid State and Structural Chemistry Unit, Indian Institute of Science, Bangalore 560 012, India*

<sup>d</sup> *Institut de Chimie, Université de Neuchâtel, Av. de Bellevaux 51, 2000 Neuchâtel, Switzerland*

## Abstract

Complexes of the general formula  $[\text{Ni}_2\text{L}_2(\mu_{1,1}\text{-N}_3)_2(\text{N}_3)_2]$  have been synthesised in good yields by reacting  $\text{Ni}(\text{NO}_3)_2 \cdot 6\text{H}_2\text{O}$  with L in the presence of excess of sodium azide in methanol at room temperature. Here L is *N,N*-bis(2-pyridylmethyl)amine ( $\text{L}^1$ ) and *N*-(2-pyridylmethyl)-*N'*,*N'*-diethylethylenediamine ( $\text{L}^2$ ). The X-ray structures of both compounds reveal that the *N,N,N* coordinating reduced Schiff bases are ligated facially. The Ni–N<sub>azido</sub>–Ni angle is  $\sim 100^\circ$  and the Ni···Ni separation is  $\sim 3.2 \text{ \AA}$ . The variable temperature magnetic susceptibility measurements of the two complexes show ferromagnetic behavior.

*Keywords:* Reduced Schiff base; Nickel; Azide; Crystal structure; Ferromagnetic

## 1. Introduction

Nickel enzymes are involved in various biological reactions [1–4] and consequently the study of the coordination chemistry of nickel has been of significant interest in recent years [5–7]. It has been demonstrated that the azido group inhibits enzymatic reactions [8,9]. Thus, the investigation of nickel–azido complexes has become a field of recent interest to understand the role of the metal ion in biological reactions. In addition, the study of such complexes has also received great deal of attention in the context of enhancement of the knowledge about magnetic interactions as well as development of magnetic materials [10–12].

Although a sizeable number of azido-bridged nickel(II) complexes have so far been reported [13–15], such complexes with reduced Schiff base ligands are rare. Herein, we describe the synthesis and characterization of two neutral end-on diazido-bridged nickel(II) complexes incorporating conformationally labile *N,N,N*-coordinating reduced Schiff bases. The single crystal X-ray structures, IR and UV–Vis spectroscopic and redox properties are discussed. The variable temperature magnetic susceptibility measurements of the complexes confirm the ferromagnetic behavior in the solid state.

## 2. Experimental

*Materials.* All the starting chemicals were analytically pure and used without further purification. The ligands were prepared according to the literature procedure [16].

\* Corresponding author. Tel.: +91 33 24146223; fax: +91 33 24146584.  
*E-mail address:* kajalrajak@hotmail.com (K.K. Rajak).

*Caution!* Azido complexes of metal ions are potentially explosive, and should be handled with care and in small amounts.

### 2.1. Physical measurements

The UV–Vis spectra were recorded on a Perkin–Elmer LAMBDA EZ-301 spectrophotometer and IR spectra were measured with a Perkin–Elmer L-0100 spectrometer. Electrochemical measurements were performed (acetonitrile solution) on a CH 620A electrochemical analyzer using a platinum electrode. Tetraethylammonium perchlorate (TEAP) [17] was used as a supporting electrolyte and the potentials are referenced to the standard calomel electrode (SCE) without junction correction. Magnetic measurements were carried out on polycrystalline samples with a Quantum Design MPMS XL SQUID susceptometer operating at a magnetic field of 0.1 T between 2 and 300 K. The diamagnetic corrections were evaluated from Pascal’s constants. Elemental analyses (C, H, N) were performed on a Perkin–Elmer 2400 Series II elemental analyzer.

### 2.2. Synthesis of the complexes

The complexes were prepared by the same general methods. Details are given here for a representative case.

$[\text{Ni}_2(\text{L}^1)_2(\mu_{1,1}\text{-N}_3)_2(\text{N}_3)_2]$  (**1**). To a methanolic solution (10 mL) of nickel(II) nitrate hexahydrate (0.146 g, 0.5 mmol) was added  $\text{L}^1$  (0.100 g, 0.5 mmol), followed by an aqueous solution of sodium azide (0.065 g, 0.10 mmol). The resulting pale green solution was stirred for 0.5 h at room temperature. Slow evaporation of the solution yielded a light green coloured crystalline product. Yield: 0.09 g, 68%. *Anal.* Calc. for  $\text{C}_{24}\text{H}_{26}\text{N}_{18}\text{Ni}_2$ : C, 42.1; H, 3.8; N, 36.84. Found: C, 41.9; H, 3.6; N, 36.6%. UV–Vis ( $\lambda_{\text{max}}/\text{nm}$  ( $\epsilon/\text{M}^{-1}\text{cm}^{-1}$ )  $\text{CH}_2\text{Cl}_2$  solution): 625(12); 1010(32). IR (KBr)/ $\text{cm}^{-1}$ :  $\nu(\text{NH})$  3010;  $\nu(\text{N}_3^-)$  2065, 2040.  $E_{\text{pa}}(\text{Ni}^{\text{III}}/\text{Ni}^{\text{II}})$ : 1.7 V.

$[\text{Ni}_2(\text{L}^2)_2(\mu_{1,1}\text{-N}_3)_2(\text{N}_3)_2]$  (**2**). Yield: 0.12 g, 68%. *Anal.* Calc. for  $\text{C}_{24}\text{H}_{42}\text{N}_{18}\text{Ni}_2$ : C, 41.1; H, 5.99; N, 35.99. Found: C, 41.4; H, 5.7; N, 36.2%. UV–Vis ( $\lambda_{\text{max}}/\text{nm}$  ( $\epsilon/\text{M}^{-1}\text{cm}^{-1}$ )  $\text{CH}_2\text{Cl}_2$  solution): 632(12); 1015(26). IR (KBr)/ $\text{cm}^{-1}$ :  $\nu(\text{NH})$  3005;  $\nu(\text{N}_3^-)$  2070, 2045.  $E_{\text{pa}}(\text{Ni}^{\text{III}}/\text{Ni}^{\text{II}})$ : 1.6 V.

### 2.3. Crystallographic studies

Suitable crystals of complexes **1** and **2** were grown by slow evaporation of their methanolic solutions. In the case of **1**, the X-ray intensity data were measured at 293 K on a Bruker AXS SMART APEX CCD diffractometer (Mo  $\text{K}\alpha$ ,  $\lambda = 0.71073$  Å). The detector was placed at a distance of 6.03 cm from the crystal. A total 606 frames were collected with a scan width of 0.3°

Table 1  
Crystallographic data for **1** and **2**

	<b>1</b>	<b>2</b>
Formula	$\text{C}_{24}\text{H}_{26}\text{N}_{18}\text{Ni}_2$	$\text{C}_{24}\text{H}_{42}\text{N}_{18}\text{Ni}_2$
Formula weight	684.04	700.18
Crystal system	monoclinic	orthorhombic
Space group	$C2/c$	$Pbca$
$a$ (Å)	19.626(4)	13.8403(5)
$b$ (Å)	11.100(2)	15.0279(5)
$c$ (Å)	14.719(3)	45.367(2)
$\beta$ (°)	101.27(3)	90.0
$V$ (Å <sup>3</sup> )	3144.6(11)	9435.9(6)
$Z$	4	12
$D_{\text{calcd}}$ ( $\text{Mg m}^{-3}$ )	1.445	1.479
$\mu$ ( $\text{mm}^{-1}$ )	1.245	1.246
Measured reflections	6604	56329
Unique reflections/ $R_{\text{int}}$	1642/0.0649	8582/0.0748
$T$ (K)	293(2)	153(2)
$R_1^a$ , $wR_2^b$ [ $I > 2\sigma(I)$ ]	0.0809, 0.2304	0.0420, 0.0856
$R_1^a$ , $wR_2^b$ [all data]	0.1086, 0.2461	0.0575, 0.0920
Goodness-of-fit on $F^2$	1.089	1.038

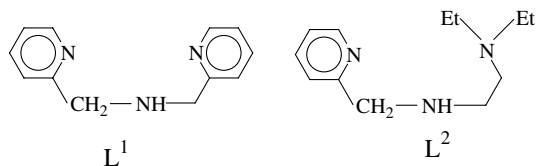
$$^a R_1 = \frac{\sum |F_o| - |F_c|}{\sum |F_o|}$$

$$^b wR_2 = \left[ \frac{\sum w(F_o^2 - F_c^2)^2}{\sum w(F_o^2)^2} \right]^{1/2}$$

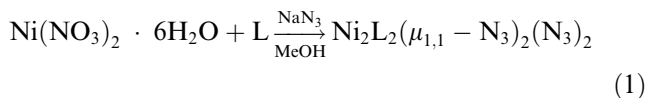
in different settings of  $\phi$ . The data were reduced in SAINTPLUS [18] and empirical absorption correction was applied using the SADABS package [18]. It was found that there was limited resolution of X-ray data in the case of **1**. For complex **2**, the intensity data were collected at 153 K on a Stoe Mark II-Image Plate Diffraction System [19] equipped with a two-circle goniometer and using Mo  $\text{K}\alpha$  graphite monochromated radiation. The image plate distance was 135 mm,  $\omega$  rotation scans 0–180° at  $\phi$  0°, and 0–42° at  $\phi$  90°, step  $\Delta\omega = 1.0^\circ$ ,  $2\theta$  range 2.7–51.2°,  $d_{\text{min}}\text{--}d_{\text{max}} = 15.03\text{--}0.82$  Å. An empirical absorption correction was applied using the DELrefABS routine in PLATON [20]. The structures were solved by direct methods using the program SHELXS-97 [21]. The refinement and all further calculations were carried out using SHELXL97 [22]. In complex **1**, the N(8) and N(9) atoms of the terminal azide group are distorted and these two were refined isotropically. The remaining non-hydrogen atoms of **1** and all the non-hydrogen atoms of **2** were refined anisotropically, using full-matrix least-squares procedures on  $F^2$ . The hydrogen atoms were included in calculated positions. Molecular structure plots were drawn using ORTEP [23]. Relevant crystal data are given in Table 1.

## 3. Results and discussion

Two reduced Schiff bases  $\text{L}^1$  and  $\text{L}^2$  (general abbreviation L) are used in this present work and these are synthesized by  $\text{NaBH}_4$  reduction of their respective Schiff bases [16].



The stoichiometric reaction of  $Ni(NO_3)_2 \cdot 6H_2O$  with  $L$  in methanol in the presence of excess of sodium azide at room temperature furnishing the pale green coloured



complexes of type  $[Ni_2L_2(\mu_{1,1}-N_3)_2(N_3)_2]$  Eq. (1).

The complexes display asymmetric azide stretches near  $2040$  and  $2070\text{ cm}^{-1}$ . The stretching frequency of  $NH$  group occurs as a broad band near  $3000\text{ cm}^{-1}$ . The complexes display an irreversible peak near  $1.6\text{ V}$  that may be assigned as a  $Ni^{II} \rightarrow Ni^{III}$  oxidation couple.

Both the complexes show two bands in  $CH_2Cl_2$  solution and the bands near  $1000$  and  $630\text{ nm}$  are believed to be of ligand field origin [24].

#### 4. Crystal structure

The crystal structures of  $[Ni_2(L^1)_2(\mu_{1,1}-N_3)_2(N_3)_2]$  (**1**), and  $[Ni_2(L^2)_2(\mu_{1,1}-N_3)_2(N_3)_2]$  (**2**) have been determined and the ORTEP diagrams are given in Figs. 1 and 2. Selected bond distances and angles are given in Tables 2 and 3. The asymmetric unit of **1** consists of one molecule while that of complex **2** contains one non-centrosymmetric and one half of a centrosymmetric molecule. In both cases, in each half of the dinuclear complexes, the tridentate ligand,  $L$  ( $L^1$ – $L^2$ ) is ligated facially and the other two equatorial sites are occupied by one termi-

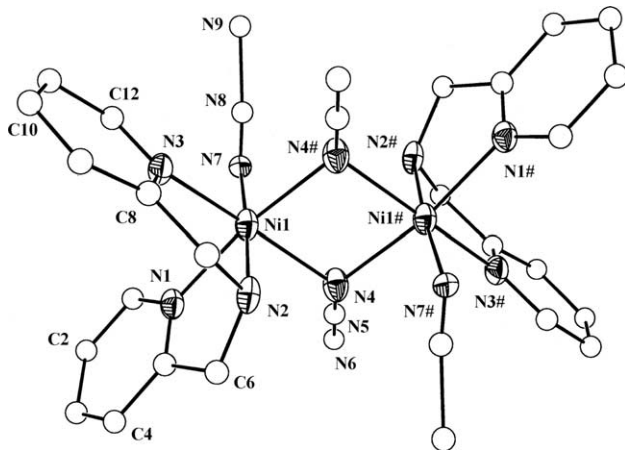


Fig. 1. Perspective view and atom labelling scheme of  $[Ni_2(L^1)_2(\mu_{1,1}-N_3)_2(N_3)_2]$  (**1**).

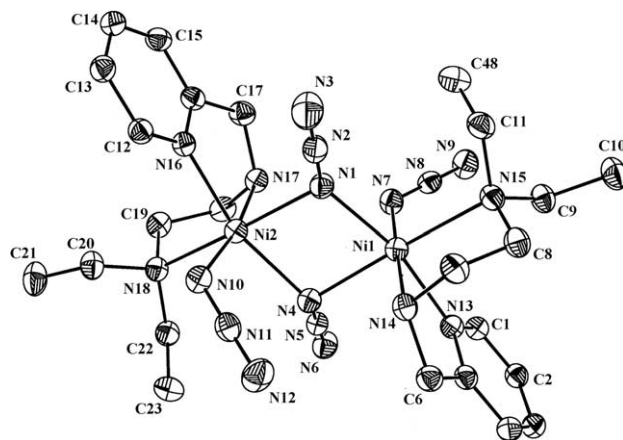


Fig. 2. Perspective view and atom labelling scheme of  $[Ni_2(L^2)_2(\mu_{1,1}-N_3)_2(N_3)_2]$  (**2**) (of one molecule).

Table 2  
Selected bond distances ( $\text{\AA}$ ) and angles ( $^\circ$ ) for **1**

Distances	
Ni(1)–N(1)	2.048(8)
Ni(1)–N(2)	2.080(8)
Ni(1)–N(3)	2.055(8)
Ni(1)–N(4)	2.086(8)
Ni(1)–N(4) #	2.088(9)
Ni(1)–N(7)	2.249(8)
Ni $\cdots$ Ni	3.191(4)
Angles	
N(1)–Ni(1)–N(2)	81.9(3)
N(1)–Ni(1)–N(3)	90.0(3)
N(1)–Ni(1)–N(4)	93.2(3)
N(1)–Ni(1)–N(4) #	170.5(4)
N(1)–Ni(1)–N(7)	93.5(3)
N(2)–Ni(1)–N(3)	80.6(4)
N(2)–Ni(1)–N(4)	88.5(3)
N(2)–Ni(1)–N(4) #	91.0(4)
N(2)–Ni(1)–N(7)	175.2(3)
N(3)–Ni(1)–N(4)	168.1(4)
N(3)–Ni(1)–N(4) #	95.1(3)
N(3)–Ni(1)–N(7)	101.0(3)
N(4)–Ni(1)–N(4) #	80.3(4)
N(4)–Ni(1)–N(7)	90.3(3)
N(7)–Ni(1)–N(4) #	93.4(3)
Ni(1)–N(4)–Ni(1) #	99.7(4)

nal and one bridging azide group. The remaining axial site of one half of the molecule is fulfilled by the equatorially coordinated azide nitrogen atom of the other half and vice versa, thus, forming a double end-on azido-bridged entity.

In the distorted  $NiN_6$  octahedral environment, the Ni–N bonds span the range  $2.043(2)$ – $2.264(2)\text{ \AA}$ . The Ni– $N_{\text{azido}}(\text{terminal})$  and the Ni– $N_{\text{azido}}(\text{end-on})$  bonds are usual [15a]. The Ni– $N_{\text{azido}}$ –Ni– $N_{\text{azido}}$  rings are planar [ $md < 0.05\text{ \AA}$ ] and the Ni– $N_{\text{azido}}$ –Ni bond angles are  $\sim 99^\circ$  and  $\sim 100^\circ$  in complexes **1** and **2**, respectively. The dihedral angle between the two bridging azido groups is  $\sim 30^\circ$  for **1** and  $\sim 25^\circ$  for **2** and the  $\mu_{1,1}$ – $N_3$  groups form an angle of  $\sim 50^\circ$  for **1** and  $\sim 40^\circ$  for **2** with

Table 3  
Selected bond distances (Å) and angles (°) for **2** (one molecule)

Distances	
Ni(1)–N(1)	2.085(2)
Ni(1)–N(4)	2.184(2)
Ni(1)–N(7)	2.077(3)
Ni(1)–N(13)	2.073(2)
Ni(1)–N(14)	2.095(3)
Ni(1)–N(15)	2.264(2)
Ni···Ni	3.222(3)
Ni(2)–N(1)	2.176(2)
Ni(2)–N(4)	2.117(2)
Ni(2)–N(10)	2.043(2)
Ni(2)–N(16)	2.072(2)
Ni(2)–N(17)	2.092(3)
Ni(2)–N(18)	2.242(2)
Angles	
N(1)–Ni(1)–N(4)	79.03(9)
N(1)–Ni(1)–N(7)	90.29(10)
N(1)–Ni(1)–N(13)	166.37(10)
N(1)–Ni(1)–N(14)	92.20(10)
N(1)–Ni(1)–N(15)	101.01(9)
N(4)–Ni(1)–N(7)	87.01(10)
N(4)–Ni(1)–N(13)	89.16(9)
N(4)–Ni(1)–N(14)	92.70(10)
N(4)–Ni(1)–N(15)	175.83(9)
N(7)–Ni(1)–N(13)	95.91(10)
N(7)–Ni(1)–N(14)	177.38(10)
N(7)–Ni(1)–N(15)	97.15(10)
N(13)–Ni(1)–N(14)	81.48(10)
N(13)–Ni(1)–N(15)	90.27(9)
N(14)–Ni(1)–N(15)	83.13(10)
Ni(1)–N(1)–Ni(2)	101.31(10)
N(1)–Ni(2)–N(4)	78.51(9)
N(1)–Ni(2)–N(10)	93.91(10)
N(1)–Ni(2)–N(16)	87.03(9)
N(1)–Ni(2)–N(17)	90.79(10)
N(1)–Ni(2)–N(18)	174.05(10)
N(4)–Ni(2)–N(10)	95.23(10)
N(4)–Ni(2)–N(16)	164.43(10)
N(4)–Ni(2)–N(17)	92.94(10)
N(4)–Ni(2)–N(18)	101.26(9)
N(10)–Ni(2)–N(16)	91.43(10)
N(10)–Ni(2)–N(17)	171.24(10)
N(10)–Ni(2)–N(18)	92.04(10)
N(16)–Ni(2)–N(17)	81.43(10)
N(16)–Ni(2)–N(18)	92.52(9)
N(17)–Ni(2)–N(18)	83.27(10)
Ni(1)–N(4)–Ni(2)	100.01(10)

the Ni–N<sub>azido</sub>–Ni–N<sub>azido</sub> plane. The terminal azide groups are quasilinear and coordinate *trans* to each other, the N–Ni···Ni–N torsion angles being 180° for **1** and 177.52(8)° and 179.47(9)° for **2**. The Ni···Ni distances in the dinuclear entities are 3.191(4) Å for complex **1** and 3.296(2) and 3.222(3) Å for **2**.

## 5. Magnetic studies

The variable temperature magnetic susceptibility measurements were carried out in the temperature range

2–300 K. The  $\chi_M T$  versus  $T$  plot for complexes **1** and **2** are given in Figs. 3 and 4. The experimental  $\chi_M T$  value is 2.6 cm<sup>3</sup> mol<sup>-1</sup> K for **1** and 2.96 cm<sup>3</sup> mol<sup>-1</sup> K for **2** at 300 K [a characteristic feature for a Ni<sup>II</sup> ion with  $g$  close to 2.30]. This value increases to 3.4 cm<sup>3</sup> mol<sup>-1</sup> K at 30 K and to 3.94 cm<sup>3</sup> mol<sup>-1</sup> K at 10 K for complexes **1** and **2**, respectively. Below 30 K (for **1**) and 10 K (for **2**) the  $\chi_M T$  values decreases abruptly to 2.4 and ~3 cm<sup>3</sup> mol<sup>-1</sup> K at 2 K. The shape of the curve is typical of intramolecular ferromagnetic coupling with the presence of either zero-field splitting ( $D$  parameter) and/or intermolecular antiferromagnetic interactions ( $J'$ ). Both  $D$  and  $J'$  are strongly correlated and show same results at low temperature. Thus, it was not possible to separate them in any attempt to fit the experimental data [25]. So two different approaches have been used to fit the experimental data for **1** and **2**: the first one was a full diagonalisation formalism introducing the single-ion  $D$  parameter employing, thus, the spin-Hamiltonian  $H = -JS_1S_1 + D[S_z^2 - 1/3S(S+1)] + g\beta HS_z$ , and the second one using the molecular field approximation, with the intermolecular  $J'$  parameter, according to the method given by Kahn with the Hamiltonian  $H = -JS_1S_1 + g\beta HS_z - zJ'(S_z)S_z$  [26]. In both the approaches, the best  $J$  values were obtained by minimizing the function  $R = \sum(\chi_M^{\text{calc}} - \chi_M^{\text{obs}})^2 / \sum(\chi_M^{\text{obs}})^2$ . By using the molecular field approach (neglecting the  $D$  parameter), the best-fit parameters obtained were as follows: complex **1**;  $J = 34.19 \pm 0.7$  cm<sup>-1</sup>,  $z'J' =$

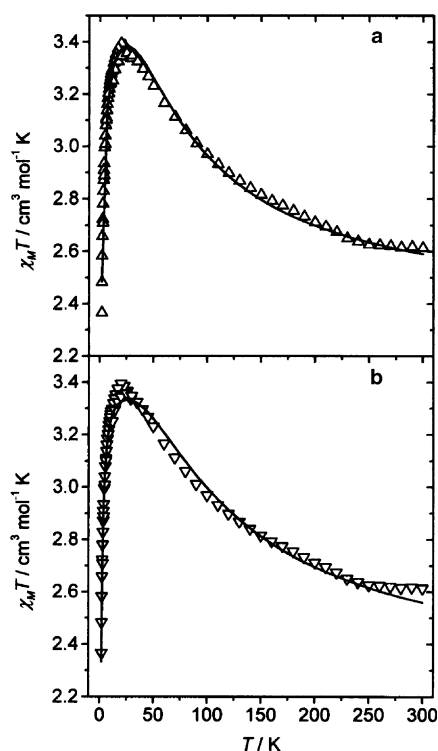


Fig. 3. Plot of  $\chi_M T$  vs.  $T$  for complex **1** (a) assuming the  $J'$  parameter without the  $D$  parameter and (b) assuming the  $D$  parameter without the  $J'$  interaction. Solid line represents the best-fit curve.

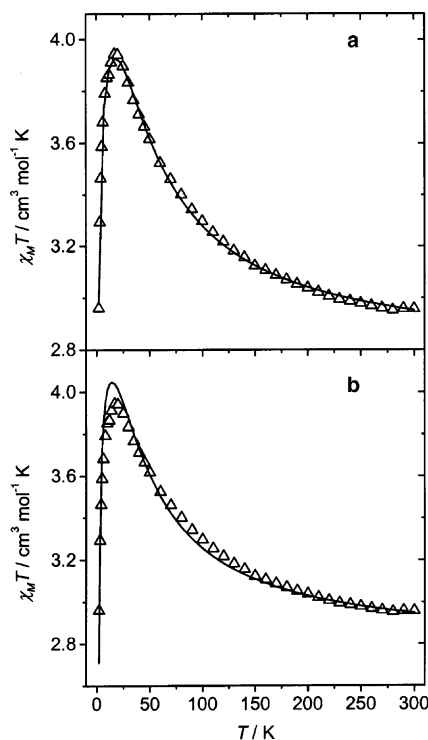


Fig. 4. Plot of  $\chi_M T$  vs.  $T$  for complex **2** (a) without considering the  $D$  parameter and with the  $z'J'$  parameter (intermolecular interactions) and (b) assuming the  $D$  parameter without the  $J'$  interaction. Solid line represents the best-fit curve.

$-0.29 \text{ cm}^{-1}$ ,  $g = 2.17 \pm 0.01$  and  $R = 6 \times 10^{-4}$  and complex **2**;  $J = 22.7 \text{ cm}^{-1}$ ,  $z'J' = -0.27 \text{ cm}^{-1}$ ,  $g = 2.35$  and  $R = 1.5 \times 10^{-4}$  (Figs. 3(a) and 4(a)). By using a full diagonalization method with the  $D$  parameter (Figs. 3(b) and 4(b)), the best-fit was obtained with the following parameters:  $J = 47.6 \pm 1 \text{ cm}^{-1}$ ,  $D = 8.4 \pm 0.5 \text{ cm}^{-1}$ ,  $g = 2.12 \pm 0.01$  and  $R = 3 \times 10^{-3}$  for complex **1** and  $J = 23.2 \text{ cm}^{-1}$ ,  $D = 5.27 \text{ cm}^{-1}$ ,  $g = 2.25$  and  $R = 1.2 \times 10^{-3}$  for complex **2**. The zero-field splitting parameters of isolated Ni(II) ions are usually large and lie in the range  $4\text{--}8 \text{ cm}^{-1}$  [27]. The plot of the reduced magnetization ( $M/N\beta$ ) is shown in Figs. 5 and 6 for complexes **1** and **2**, respectively. For complex **1**, this curve is in good agreement with the theoretical Brillouin function for two isolated nickel(II) ions assuming  $g = 2.13$  (average of the two different fits). The coincidence of the curve can be attributed to the positive  $J$  value and the negative  $J'$  and  $D$  parameters having an opposite effect. The curve of reduced magnetization does not follow the Brillouin formula in the case of **2**. At low fields, the experimental points are above the theoretical ones but at high fields, the experimental points lie below the theoretical curve. This feature is indicative of the complication due to the  $D$  parameter and the presence of ferromagnetic and anti-ferromagnetic interactions.

It is stated in the literature [12,28] that for a bis( $\mu_{1,1}$ - $\text{N}_3$ ) bridged dinuclear nickel(II) system the strength of

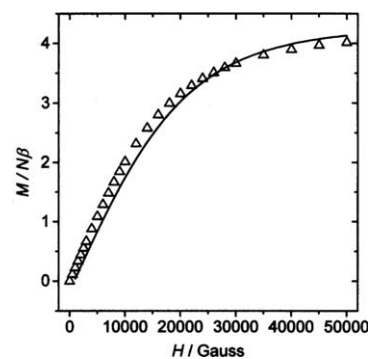


Fig. 5. Plot of the reduced magnetization ( $M/N\beta$ ) vs.  $H$  at 2 K for **1**. Solid line represents the Brillouin function for two isolated  $\text{Ni}^{2+}$  ions with  $g = 2.13$ .

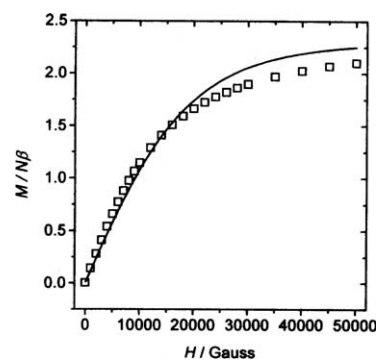


Fig. 6. Plot of the reduced magnetization ( $M/N\beta$ ) vs.  $H$  at 2 K for **2**. Solid line represents the Brillouin formula for  $g = 2.35$ .

ferromagnetic coupling between two paramagnetic centers mainly depends on the Ni–N<sub>azido</sub>–Ni angle, the average angle being close to  $101^\circ$ . With this and similar angles the coupling is ferromagnetic. In **1**, this angle is  $\sim 99^\circ$  and in **2** it is  $\sim 100^\circ$ . The Ni–N<sub>azido</sub> and Ni $\cdots$ Ni distances are  $\sim 2.085$  and  $\sim 3.191 \text{ \AA}$  for **1** and  $\sim 2.12$  and  $\sim 3.22 \text{ \AA}$  for **2**, respectively. Thus the structural parameters corroborate the observed ferromagnetic interactions in the two complexes.

In the solid state, in complex **2** the N(14)–H(14) and N(17)–H(17) groups are involved in intramolecular hydrogen bonding with N(12) and N(7) atoms, respectively. The intramolecular hydrogen bonding could originate a small but not negligible coupling into the magnetic exchange interaction. Hence, the weak coupling generated by such hydrogen bonding may modify the overall Ni–N<sub>azido</sub>–Ni coupling in case of complex **2**.

## 6. Conclusion

Two new complexes of the formula  $[\text{Ni}_2(\text{L}^1)_2(\mu_{1,1}\text{-N}_3)_2(\text{N}_3)_2]$  (**1**) and  $[\text{Ni}_2(\text{L}^2)_2(\mu_{1,1}\text{-N}_3)_2(\text{N}_3)_2]$  (**2**) have been synthesized and characterized. These species represent the first examples of an end-on azido bridged dinuclear entity incorporating conformationally flexible reduced Schiff base ligands. Variable temperature magnetic

moment measurements of the two complexes confirm the ferromagnetic behavior in the solid state and in the case of **2**, the intramolecular hydrogen bonding modulates the overall Ni–N<sub>azido</sub>–Ni coupling. Our search for new nickel(II) complexes with different reduced Schiff base ligands and the study of their solid state behavior is in progress.

## 7. Supporting Information

Crystallographic data for structural analysis have been deposited with the Cambridge Crystallographic Data Centre with CCDC numbers 272898 and 246819 for **1** and **2**, respectively. Copies of this information may be obtained free of charge from the Director, CCDC, 12 Union Road, Cambridge CB2 1EZ, UK, fax: +44 1223 336 033, or e-mail: [deposit@ccdc.cam.ac.uk](mailto:deposit@ccdc.cam.ac.uk) or [www: http://www.ccdc.cam.ac.uk](http://www.ccdc.cam.ac.uk).

## Acknowledgments

Financial support from the Council of Scientific and Industrial Research, New Delhi, India and from the Department of Science and Technology, New Delhi, India are gratefully acknowledged. We are also thankful to DST for the data collection on the CCD facility setup (Indian Institute of Science, Bangalore, India) under the IRHPA-DST program. Joan Ribas acknowledges the financial support from the Spanish Government (Grant BQU2000/0791).

## References

- [1] J.R. Lancaster, Jr. (Ed.), *The Bioinorganic Chemistry of Nickel*, VCH Publishers, New York, 1998.
- [2] M.A. Halcrow, G. Christou, *Chem. Rev.* 94 (1994) 2421.
- [3] T.I. Doukov, T.M. Iverson, J. Seravalli, S.W. Ragsdab, C.L. Drenman, *Science* 298 (2002) 567.
- [4] J. Wuerges, J.-W. Lee, Y.-I. Yim, H.-S. Yim, S.-O. Kang, K.D. Carugo, *Proc. Natl. Acad. Sci. USA* 101 (2004) 8569.
- [5] S. Akine, T. Nabeshima, *Inorg. Chem.* 44 (2005) 1205.
- [6] N. Sprutta, S.P. Rath, M.M. Olmstead, A.L. Balch, *Inorg. Chem.* 44 (2005) 1452.
- [7] C.-M. Lee, C.-H. Chen, S.-C. Ke, G.-H. Lee, W.-F. Liaw, *J. Am. Chem. Soc.* 126 (2004) 8406.
- [8] H.-D. Youn, E.-J. Kim, J.-H. Roe, Y.C. Hah, S.-O. Kang, *Biochem. J.* 318 (1996) 1452.
- [9] R.K. Watt, P.W. Ludden, *J. Bacteriol.* 181 (1999) 4554.
- [10] (a) A. Escuer, R. Vicente, J. Ribas, M.S. El Fallah, X. Solans, M. Font-Bardía, *Inorg. Chem.* 32 (1993) 3727;  
(b) M. Monfort, I. Resino, J. Ribas, X. Solans, M. Font-Bardía, *New J. Chem.* 25 (2001) 1577.
- [11] (a) M.-F. Charlot, O. Kahn, M. Chaillet, C. Larrieu, *J. Am. Chem. Soc.* 108 (1986) 2574;  
(b) L.K. Thompson, S.S. Tandon, M.E. Manuel, *Inorg. Chem.* 34 (1995) 2356.
- [12] E. Ruiz, J. Cano, S. Alvarez, P. Alemany, *J. Am. Chem. Soc.* 120 (1998) 11122.
- [13] (a) R.J. Butcher, C.J. O'Connor, E. Sinn, *Inorg. Chem.* 21 (1982) 616;  
(b) S. Sikorav, I. Bkouche-Waksman, O. Kahn, *Inorg. Chem.* 23 (1984) 490;  
(c) R. Vicente, A. Escuer, J. Ribas, M.S. El Fallah, X. Solans, M. Font-Bardía, *Inorg. Chem.* 32 (1993) 1920.
- [14] (a) M. Monfort, I. Resino, J. Ribas, H. Stoeckli-Evans, *Angew. Chem., Int. Ed. Engl.* 39 (2000) 191;  
(b) M. Monfort, I. Resino, M.S. El Fallah, J. Ribas, X. Solans, M. Font-Bardía, H. Stoeckli-Evans, *Chem. Eur. J.* 7 (2001) 280;  
(c) S. Martin, M.G. Barandika, L. Lezama, J.L. Pizzaro, Z.E. Serna, J.I.R. de Larramendi, M.I. Arriortua, T. Rojo, R. Cortes, *Inorg. Chem.* 40 (2001) 4109;  
(d) A. Escuer, R. Vicente, F.A. Mautner, M.A.S. Goher, M.A.M. Abu-Youssef, *Chem. Commun.* (2002) 64.
- [15] (a) S. Deoghoria, S. Sain, M. Soler, W.T. Wong, G. Christou, S.K. Bera, S.K. Chandra, *Polyhedron* 22 (2003) 257;  
(b) S.K. Dey, N. Mondal, M.S. El Fallah, R. Vicente, A. Escuer, X. Solans, M. Font-Bardía, T. Matsushita, V. Gramlich, S. Mitra, *Inorg. Chem.* 43 (2004) 2427.
- [16] S. Larsen, K. Michelsen, E. Pedersen, *Acta Chem. Scand. Sect. A* 40 (1986) 63.
- [17] G.K. Lahiri, S. Bhattacharya, B.K. Ghosh, A. Chakravorty, *Inorg. Chem.* 26 (1987) 4324.
- [18] SMART, SAINT, SADABS, XPREP, SHELXTL, Bruker AXS Inc., Madison, WI, 1998.
- [19] X-Area V1.17 & X-RED32 V1.04 Software, Stoe & Cie GmbH, Darmstadt, Germany, 2002.
- [20] A.L. Spek, *J. Appl. Crystallogr.* 36 (2003) 7.
- [21] G.M. Sheldrick, SHELXS97, Program for Crystal Structure Determination, *Acta Crystallogr., Sect. A* 46 (1990) 467.
- [22] G. Sheldrick, SHELXL97, Universität Göttingen, Göttingen, Germany, 1999.
- [23] C.K. Johnson, ORTEP, Report ORNL-5138, Oak Ridge National Laboratory, Oak Ridge, TN, 1976.
- [24] (a) G. Zakrzewski, L. Sacconi, *Inorg. Chem.* 7 (1968) 1034;  
(b) P. Bamfield, R. Price, R.G.J. Miller, *J. Chem. Soc., Sect. A* (1969) 1447.
- [25] A.P. Ginsberg, R.L. Martin, R.W. Brookes, R.C. Sherwood, *Inorg. Chem.* 11 (1972) 2884.
- [26] O. Kahn, *Molecular Magnetism*, VCH, New York, 1993.
- [27] R. Boča, *Coord. Chem. Rev.* 248 (2004) 757.
- [28] J. Ribas, A. Escuer, M. Monfort, R. Vicente, R. Cortes, L. Lezama, T. Rojo, *Coord. Chem. Rev.* 193–195 (1999) 1027.